Petrus ML, Hu Y, Moia D, Calado P, Leguy A, Barnes PRF, Docampo P.
The Influence of Water Vapor on the Stability and Processing of Hybrid Perovskite Solar Cells Made from Non-Stoichiometric Precursor Mixtures.
***ChemSusChem* 2016, 9(18), 2699-2707**

The influence of water vapor on the stability and processing of hybrid perovskite solar cells made from non-stoichiometric precursor mixtures

Michiel L. Petrus,[1,†] Yinghong Hu,[1,†] Davide Moia,[2] Philip Calado,[2] Aurélien M. A. Leguy,[2] Piers R. F. Barnes,[2,] Pablo Docampo[1,*]*

[†] These authors contributed equally to this work

[1] Department of Chemistry, LMU Munich, Munich, Germany, 81377

[2] Physics Department, Imperial College London, London, United Kingdom, SW7 2AZ

e-mail: piers.barnes@imperial.ac.uk, pablo.docampo@cup.lmu.de

Keywords: non-stoichiometric, MAI excess, PbI_2 excess, hydration, stability

Abstract

We investigated the influence of moisture on $CH_3NH_3PbI_3$ perovskite films and solar cells derived from non-stoichiometric precursor mixtures. We followed both the structural changes under controlled air humidity *via in-situ* X-ray diffraction, and the electronic behavior of devices prepared from these films. A small PbI_2 excess in the films improved the stability of the perovskite compared to stoichiometric samples. We assign this to excess PbI_2 layers at the perovskite grain boundaries or to the termination of the perovskite crystals with lead and iodine. In contrast, the MAI-excess films composed of smaller perovskite crystals showed increased electronic disorder and reduced device performance due to poor charge collection. Upon exposure to moisture followed by dehydration ("solvent annealing"), these films recrystallized to form larger, highly oriented crystals with fewer electronic defects and a remarkable improvement in photocurrent and photovoltaic efficiency.

1. Introduction

In the past few years hybrid lead halide perovskites have emerged as a promising material for photovoltaic applications due to their outstanding optoelectronic properties.[1–3] The abundance of the precursor materials and the possibility of solution processing raises the hope of low-cost, highly efficient solar cells with a short energy payback time compared to currently established technologies.[4–8]

The Achilles heel of hybrid perovskite photovoltaic devices is their poor stability, especially under operating conditions, creating a considerable barrier to commercialization of the technology.[9] Beside environmental factors such as thermal stress and UV-light irradiation in air,[9–11] humidity-induced changes

to the perovskite structure have been identified as one of the major degradation pathways which strongly affects device lifetime.[12,13] Degradation upon exposure to moisture has so far only been suppressed by physical encapsulation or through the introduction of organic or inorganic passivation layers[14–16] which may place constraints on device performance. Fully understanding the effect of water on perovskite processing and degradation is thus important to formulate new solutions to this challenge.

The influence of humid air on hybrid perovskite films has been investigated by several groups. We have recently reported the formation of intermediate hydrate crystals as first degradation products of the perovskite, followed by their irreversible decomposition into PbI_2.[17] In general, the hygroscopic and volatile nature of the organic compound, methylammonium iodide (MAI), is understood as the weak spot of the perovskite crystal, leading to water ingress and film degradation.[18–20] To date, most of the stability studies have been performed on perovskite films fabricated from stoichiometric precursor solutions (PbI_2:MAI in 1:1 molar ratio) or with an excess of MAI.[17,21–23] However, recently reported champion perovskite solar cells showing power conversion efficiencies (PCE) exceeding 20% contain a 5–10% molar excess of PbI_2.[24–28] The remnant PbI_2 excess within the final absorber layer is believed to improve perovskite crystallization and to reduce non-radiative recombination rates by passivation of crystal grain boundaries, which could explain the additional boost in PCE.[24,29–32]

While the community agrees on the beneficial effect of a small PbI_2 excess in the perovskite layer on device performance, little is known about the moisture-stability of these non-stoichiometric perovskite films. Previously, Liu *et al.*[31] and Zhang *et al.*[33] prepared methylammonium lead iodide films *via* a two-step sequential deposition method to study the stability of these samples. In both cases, the incomplete conversion of PbI_2 into the perovskite phase leads to a residual PbI_2 interlayer between TiO_2 and perovskite, which is reported to accelerate the film degradation upon exposure to humidity. However, state-of-the-art devices are mostly derived from a one-step deposition method, where the perovskite precursor mixture is spin-coated on the substrate, followed by an “anti-solvent dripping” step to initialize crystal nucleation. Clearly, different fabrication protocols may result in different locations and morphologies of the PbI_2 excess within the device. This is likely to have a substantial effect on the degradation kinetics occurring within the perovskite film. Therefore, elucidating the link between PbI_2 passivation, moisture-induced processing and degradation effects is important to maximize both device efficiency and stability.

In this work, we studied the effect of moisture on methylammonium lead iodide ($MAPbI_3$) films derived from non-stoichiometric perovskite precursor mixtures, *i.e.* perovskite films containing a small excess of PbI_2 or MAI. We inferred the location of the initial PbI_2 excess within the perovskite film through X-ray diffraction (XRD) experiments. In order to improve the understanding of the degradation mechanism, we performed *in-situ* XRD measurements under controlled humidity levels in air (see Figure S1). In contrast to previous reports, our results indicate that a small PbI_2 excess decelerates the decomposition of the perovskite film upon exposure to moisture compared to a stoichiometric perovskite film. Additionally, we found that devices containing an MAI excess first show very low PCEs due to small perovskite crystals sizes. These are likely to be surrounded by MAI-rich regions with a high concentration of electronic defects which impede charge collection. However, the performance of devices made from MAI-excess solutions is significantly improved after a short exposure of the films to humidity at room temperature. This results

in recrystallization, grain reorientation and the removal of electronic disorder from the perovskite layer – a process which we can regard as a form solvent annealing with water vapor. Our findings are, in principle, also applicable to mixed cation/halide systems as these films are also deposited from non-stoichiometric mixtures.[34] In this case we expect a similar effect upon exposure to moisture as the typical cations used, formamidinium and cesium, are also hygroscopic and will likely undergo a similar enhanced mobility in the presence of water.

2. Results and Discussion

2.1 Effect of the hydration on the perovskite structure

In order to study the effect of the precursor stoichiometry on the stability of the perovskite structure, we prepared perovskite thin films which incorporated a 5% molar excess of MAI in the precursor solution, a stoichiometric mixture, and one incorporating a 5% molar excess of PbI_2; these samples are termed "MAI-excess", "stoichiometric" and "PbI_2-excess" in the following. The 1.25 M stoichiometric precursor solution was obtained by dissolving PbI_2 and MAI in a 1:1 molar ratio in a *N*,*N*-dimethylformamide (DMF): dimethyl sulfoxide (DMSO) solvent mixture. The corresponding amount of solid MAI or PbI_2 was then added to the stoichiometric perovskite solution to yield the MAI-excess and PbI_2-excess solutions, respectively. By employing an anti-solvent assisted one-step deposition method similar to the previously reported protocol for state-of-the-art devices,[24,26,35] a comparable distribution of the precursor excess within the perovskite layer can be expected. In short, the perovskite solution is spin-coated onto a substrate, followed by chlorobenzene dripping to induce crystal nucleation. After annealing on a hotplate, the crystallization is complete and uniform, shiny perovskite films were obtained.

Figure S2 shows the XRD patterns of the three different freshly prepared perovskite films. No significant differences in the intensity of the typical diffraction peaks originating from the tetragonal $MAPbI_3$ phase were observed. The expected (001) PbI_2 reflection at the 2θ value of 12.6° is obvious for the PbI_2-excess film, whereas it is not present in the other two samples. Previous studies report that the excess PbI_2 is located near the substrate,[31] however, its distribution strongly depends on the fabrication route. To infer the location of the PbI_2 excess within our absorber layer, we performed grazing-incidence XRD measurements at different incidence angles in the range of 0.3°–2.5°, as presented in Figure S3. At incidence angles of 0.6° and lower, the X-ray scattering depth is smaller than the total film thickness of 320 nm, thereby providing information about the distribution of the PbI_2 excess within the perovskite layer.[36] Our results show that at an incidence angle of 0.3°, the (001) peak of PbI_2 is still present in the diffractogram, indicating that the excess PbI_2 is not solely accumulated at the perovskite/TiO_2 interface but distributed throughout the entire perovskite film.

Furthermore, monitoring the crystallization process of the non-stoichiometric perovskite layer can provide an insight into the formation and distribution of the excess PbI_2.[37] We performed *in-situ* XRD measurements during the annealing process of a freshly deposited perovskite film prepared from a PbI_2 excess solution (Figure 1). Initially, we only observe the diffraction peaks assigned to the previously reported intermediate MAI-PbI_2-DMSO complex.[38,39]During the first annealing step at 40 °C the

reflections of this MAI-PbI_2-DMSO complex become more narrow, indicating the growth of the intermediate phase crystals. At the same time, characteristic reflections of the $MAPbI_3$ phase (*e. g.* at 2θ = 14.1° and 28.3°) appear. Upon further annealing, the perovskite peaks increase in intensity while the intensity of the MAI-PbI_2-DMSO reflections simultaneously decrease, suggesting the formation of $MAPbI_3$ crystals from the intermediate phase as DMSO is released. During the second annealing step at 100 °C, the last remaining solvent was removed from the film, after which the excess PbI_2 crystallized. Since the small amount of excess PbI_2 crystallizes only at the very end of the annealing procedure, we propose that PbI_2 is present at the grain surface of the previously formed perovskite crystals. This finding is in agreement with the incidence angle-dependent XRD measurements in Figure S3. Additionally, since the PbI_2 excess stays solvated until the final stage of the crystallization process, it is likely that this has an influence on the $MAPbI_3$ crystal termination.

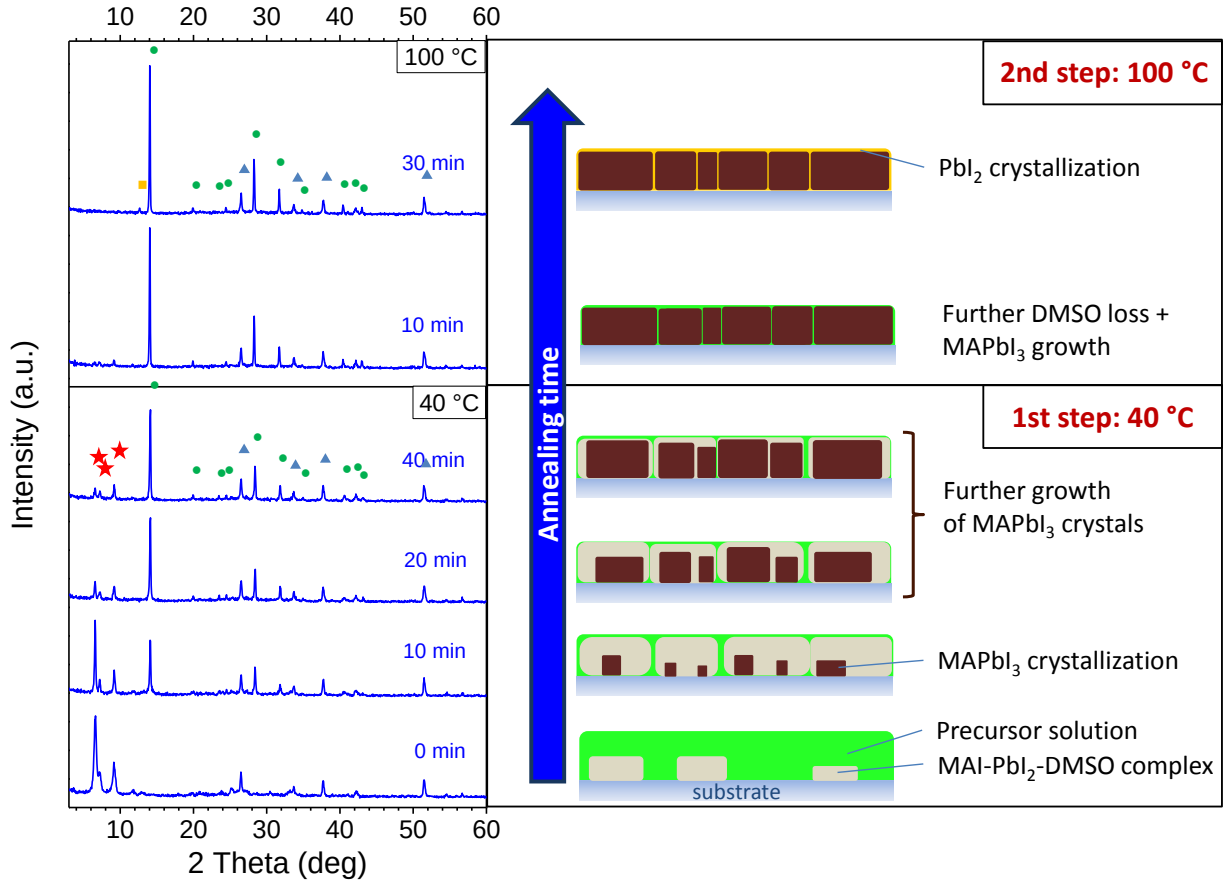

Figure 1. In-situ XRD measurement during the annealing of a freshly spin-coated $MAPbI_3$ film prepared from a perovskite solution with 5 mol% PbI_2 excess. In the first step, the film was annealed for 40 min at 40 °C followed by a second step at 100 °C. The right panel shows a schematic representation of the crystal formation inferred from the XRD measurements. Initially, the MAI-PbI_2-DMSO complex (red stars in the XRD pattern) is formed, followed by the $MAPbI_3$ crystals (green dots) and at the end, after complete removal of the solvents, crystalline PbI_2 can be observed (yellow square).

Using XRD techniques to determine the location of a small MAI excess within the corresponding perovskite films is difficult as the diffraction intensity for MAI is relatively low. Since the same fabrication method is used for all samples, we expect the excess MAI to be also distributed homogeneously between the preformed $MAPbI_3$ crystals, presumably at the grain boundaries as reported by Son *et al*.[35]

Previous studies report the detrimental effect of residual PbI_2 material at the perovskite/TiO_2 interface on the film stability towards humidity.[31] Here, we investigate the influence of moisture on perovskite films with a more homogeneous distribution of the precursor material excess which is more comparable to the absorber layers used in state-of-the-art devices showing high efficiencies. In order to compare the moisture stability of the three $MAPbI_3$ films with different precursor stoichiometry, we exposed the samples to air with a constant relative humidity (RH) of 90% in a closed chamber at room temperature. We followed the changes in the composition of the films with *in-situ* XRD measurements at regular intervals, as presented in Figure 2. Our results show that the stoichiometry of the precursor mixture critically affects the timescale of structural changes as well as the nature of the degradation products.

For the perovskite films with a stoichiometric ratio of precursors we found that PbI_2 is initially formed as a degradation product (Figure 2). With prolonged exposure to humidity, the characteristic reflections of the monohydrated $MAPbI_3$ ($CH_3NH_3PbI_3{\cdot}H_2O$) at the 2θ values 8.6° and 10.5° appear. Interestingly, the formation of additional PbI_2 as a result of degradation in the PbI_2-excess sample is significantly slower in comparison to the stoichiometric perovskite film. Similarly, we observed the crystalline monohydrate phase after 90 min in the stoichiometric samples, while for the PbI_2-excess sample, the characteristic reflections of the monohydrate only appeared after 180 min. We compared the difference in the degradation rate between the stoichiometric and the PbI_2-excess samples by plotting the ratio between the (001) peak of PbI_2 at 12.6° and the (110) peak of the perovskite at 14.1° (Figure S4). Since we observe that perovskite crystal reorientation is similar and relatively minor for both samples, the graph indicates that the formation of PbI_2 in the stoichiometric sample is significantly faster than in the PbI_2-excess sample. We found that for both films, the monohydrate forms at a PbI_2:$MAPbI_3$ peak intensity ratio of around 3:4.

In contrast, the MAI-excess sample does not show the formation of PbI_2 within the timescales studied. Surprisingly, during the first 60 min of exposure time, the XRD pattern does not exhibit any degradation products at all. Instead, the remarkable increase in the (110) and (220) reflections of $MAPbI_3$ indicate an improvement in crystallinity for the perovskite phase. After more than 60 min, the reflections of the monohydrate $CH_3NH_3PbI_3{\cdot}H_2O$ appear in the diffraction pattern, which is in accordance with previously reported results by Leguy *et al.* where a 0.4% MAI molar excess was used to form the $MAPbI_3$ film.[17] Recent calculations suggest that the monohydrate phase should thermodynamically be stable at high relative humidities at room temperature.[20] These calculations also show that a dihydrate structure of the perovskite ($(CH_3NH_3)_4PbI_6 \cdot 2H_2O$) can form at lower relative humidities. However, this phase appears to be thermodynamically unstable relative to PbI_2 and MAI which may explain why it did not appear in the present study, since it is likely that it will only be observed under kinetically favorable conditions.

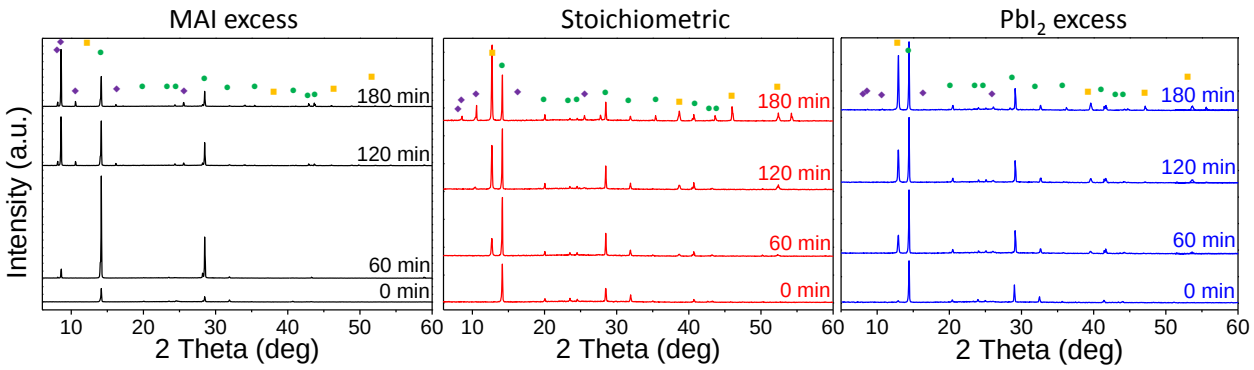

Figure 2. In-situ XRD measurements of the hydration of perovskite films prepared from solutions with different precursor ratios. The films were exposed to 90% RH in air for 0–180 min. The positions of the XRD peak for $MAPbI_3$ (green circles), PbI_2 (yellow squares) and $CH_3NH_3PbI_3{\cdot}H_2O$ (purple diamonds) are marked in the graphs.

Scanning electron microscopy (SEM) cross-section images of the different perovskite films reveal the effect of hydration on the crystal morphology (Figure 3). For both stoichiometric and PbI_2-excess samples, we observe small protrusions over the crystals after exposure to humidity, which might originate from partial degradation of the perovskite crystals. In the case of MAI-excess we find no such protrusions, indicating a different process during the exposure to humidity. Initially, the film is composed of relatively small and irregularly shaped crystals. However, after a short hydration process at 90% RH, the previously small crystallites have since recrystallized to form large crystals. This observation is consistent with the increased intensities of the (110) and (220) perovskite diffraction peaks (Figure 2), suggesting higher crystallinity and a more preferential crystal orientation.

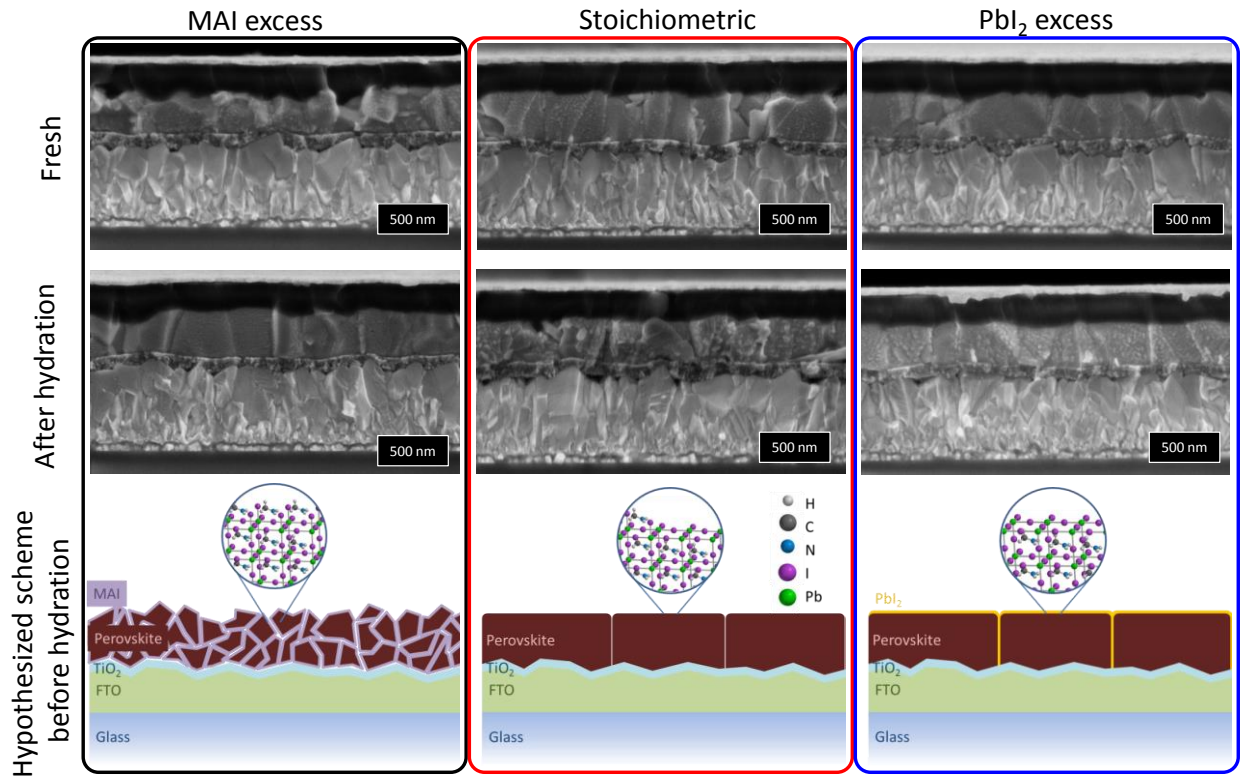

Figure 3. SEM cross-section of photovoltaic devices with a $MAPbI_3$ perovskite layer prepared with different precursor ratios. Top figures show SEM cross-sections of freshly prepared devices and figures below show the samples after exposure to 90% RH for 45 min before applying spiro-OMeTAD. The bottom images depict a schematic representation of the morphology of the perovskite film before hydration with an inset showing the hypothesized crystal surface termination for the perovskite grains at an atomic level. We note that water will be removed from these films by the SEM evacuation process.

These results strongly indicate that the precursor ratio during the perovskite film formation affects how water penetrates the perovskite crystals/films. We will discuss each case separately:

First, $MAPbI_3$ films fabricated with a PbI_2 excess exhibit markedly slower degradation dynamics and no immediate formation of hydrated perovskite species. We consider two possible mechanisms by which the initially PbI_2 excess protects the perovskite against moisture: (I) a PbI_2 layer at the grain boundaries functions as a barrier against water infiltration, and/or (II) the excess of PbI_2 facilitates the termination of the perovskite crystals with lead and iodine atoms, preventing water ingress into the crystals. The first argument considers that, unlike MA^+ ions in $MAPbI_3$,[19] PbI_2 lacks strong hydrogen-bonding interactions with water molecules and therefore can be considered as a passivation layer. The second option is in agreement with computational studies performed by Mosconi *et al.*,[40] where the authors predict that

PbI_2-terminated perovskite crystals are more robust against moisture-induced degradation than MAI-terminated surfaces. They also show that defects in the PbI_2-terminated slab are the initiation point for degradation of the perovskite, from which cavities can grow by gradual ingress of water molecules, allowing further decomposition of the perovskite. For clarification we illustrated these hypotheses schematically in Figure 3.

Second, stoichiometric $MAPbI_3$ films show relatively fast formation of PbI_2 and $CH_3NH_3PbI_3{\cdot}H_2O$ upon exposure to a high level of humidity. SEM cross-section images (Figure 3) do not display any significant difference in crystal size between the stoichiometric and PbI_2-excess films, which is in agreement with literature.[25] This indicates that the faster degradation of the stoichiometric films is not merely the result of an increase in total grain surface which is exposed to humidity. It is noteworthy that the PbI_2 obtained as a result of degradation does not seem to protect the perovskite against humidity-induced degradation in the same way as the PbI_2 excess which was added to the precursor solution.

Third, the XRD patterns of the MAI-excess films exhibit a remarkable increase in the (110) and (220) reflections of the perovskite phase without any signs of degradation during the first 60 min (Figure 4a). Yang *et al.*[23] report the same increase in the respective XRD signals by annealing an MAI-excess $MAPbI_3$ film in air under ambient conditions. The authors assign the reformation of the $MAPbI_3$ crystals to the diffusion of MA^+ and I^- from MAI reservoirs into the thermally created vacancies. The dynamic perovskite-formation process allows the growth of large grains with high crystallinity and strong orientation along the (110) direction. We expect a comparable self-healing process to occur in our films during exposure to humid air. The infiltrated water degrades the perovskite under the evolution of methylamine and HI which are volatile and can escape the film. The MA^+ and I^- vacancies which are created as a result of the hydration can be refilled by the excess MAI. According to computational studies by Tong *et al.* and Mosconi *et al.*, MAI-terminated perovskite surfaces are prone to the infiltration of water molecules which can strongly affect the perovskite structure.[40,41] With this in mind, we suggest that water molecules penetrating the perovskite structure could increase the precursor mobility and allow the perovskite to recrystallize and reorient during the first 60 min (Figure 4c). This is supported by the SEM images, verifying the significant change in crystal morphology.

Figure 4b depicts the evolution of the (110) peak intensity relative to the (121) or (022) reflections with increasing hydration time. The highest relative intensity for the (110) diffraction peak can be found after 50 min, followed by a steady decrease upon longer exposure times. The employed fabrication route of the perovskite films already leads to a preferential orientation along the (110) planes. During the moisture-assisted recrystallization, this dominating orientation seems to dictate the direction in which the large crystals will emerge. Our observations indicate that, once the reservoir of excess MAI has been consumed, no further reorganization of the perovskite film due to the self-healing process takes place and degradation is initialized by the formation of the hydrated perovskite species.

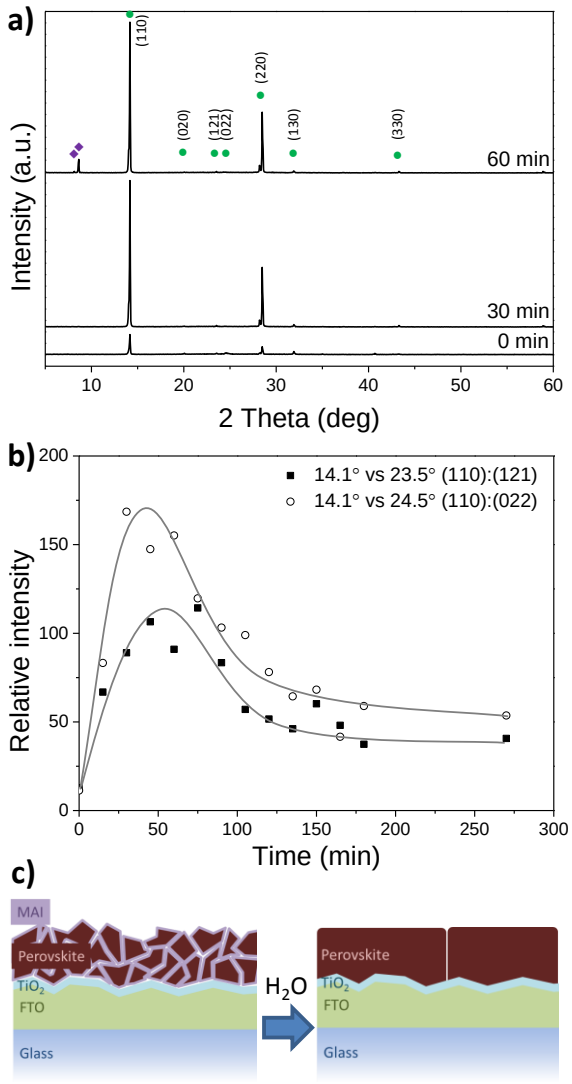

Figure 4. In-situ XRD measurements monitoring the hydration of a perovskite film prepared with a 5 mol% excess of MAI. (a) XRD patterns of the perovskite film during the first hour of exposure to 90% RH. The $MAPbI_3$ peaks are labelled with green circles and the monohydrate peaks with purple diamonds. (b) Relative intensities of the (110) perovskite peak (2θ = 14.1°) over the (121) and (022) orientations (2θ = 23.5 and 24.5°) as a function of time showing that the perovskite crystals become more oriented in the first hour of exposure to 90% RH. The grey lines are drawn as a guide to the eye. (c) Schematic representation of the change in morphology of the $MAPbI_3$ crystals after the hydration/dehydration treatment.

2.2 Effect of hydration on perovskite solar cells

In order to investigate the effect of precursor stoichiometry on the photovoltaic performance before and after exposure of the $MAPbI_3$ perovskite layer to moisture, we fabricated perovskite solar cells with the

following planar device architecture: fluorine-doped tin oxide (FTO)/compact TiO_2/$MAPbI_3$/spiro-OMeTAD/Au. We prepared different perovskite layers employing non-stoichiometric mixtures and the same method as for the thin films. Consistent with reports by several other groups,[24,25] we found that a small excess of PbI_2 (2–10 mol%) in the perovskite precursor solution increases the photovoltaic performance of the as-prepared devices (Figure S5). An optimized recipe using 5 mol% PbI_2 excess results in devices with an average PCE = 13.5% (Figure 5) compared to stoichiometric $MAPbI_3$ samples (average PCE = 11.4%). In contrast, we found that an excess of MAI is detrimental for the device performance, resulting in power conversion efficiencies of only 4.7% on average, mainly due to a loss in short-circuit current density (J_{sc}). UV-Vis absorption and spectroscopic ellipsometry measurements show that the lower J_{sc} does not originate from a reduced absorption of the film, which was found to be comparable for the different samples (Figure S6 and S7). We estimated the reported device characteristics from the measured *J-V* curves obtained from the reverse scan (from V_{oc} to J_{sc}). All as-prepared devices exhibit a comparable degree of hysteresis between the forward and reverse scans (Figure S8 and S9).

To examine the effects of moisture on the films before they were fabricated into solar cells the perovskite films were stored in air with a controlled humidity of 75% RH in a closed chamber at room temperature. We note that the substrate underneath the perovskite film can influence the time-scale of hydration effects.[31,42,43] For this reason, the time-scale of degradation in perovskite films prepared on glass/FTO/TiO_2 substrates is not directly comparable to samples on glass substrates. After the hydration procedure, we transferred the samples to a nitrogen-filled glovebox and deposited spiro-OMeTAD as hole transporting layer, followed by thermally evaporating 40 nm thick gold electrodes under high vacuum. Our previous studies suggest that any monohydrate crystals which may have formed are likely to undergo dehydration and reconvert into the perovskite phase during these low humidity processing steps (note that this dehydration process will also have occurred for the films examined in the SEM in Figure 3).[17]

The photovoltaic performance of devices comprising stoichiometric and PbI_2-excess films is slightly lower after exposure at 75% RH for 1 h (Figure 5) relative to devices made from films that have not been exposed to moisture. During this relatively short exposure, an additional ~5 mol% PbI_2 was built up in the films as a degradation product (Figure S10 and S11). We consider this to be the reason for the loss in performance. Curiously, the PbI_2 which originates from degradation does not seem to improve the photovoltaic performance as we observed for the devices made by using a PbI_2 excess in the film preparation. This suggests that the PbI_2 formed upon hydration has a different (and detrimental) spatial distribution or orientation relative to the PbI_2 excess which is added during the film preparation. It is known that PbI_2 exhibits an anisotropic electrical conductivity, which could function as a barrier for charge carriers, depending on the crystal orientation.[44,45] Upon longer exposure of the films to humidity (12 h), a further decrease in the performance of the resulting devices for both types of samples indicates further degradation. Despite the slower decomposition of the PbI_2-excess sample in the *in-situ* XRD measurements, we do not observe a large difference in the loss in performance between the stoichiometric and the PbI_2-excess devices.

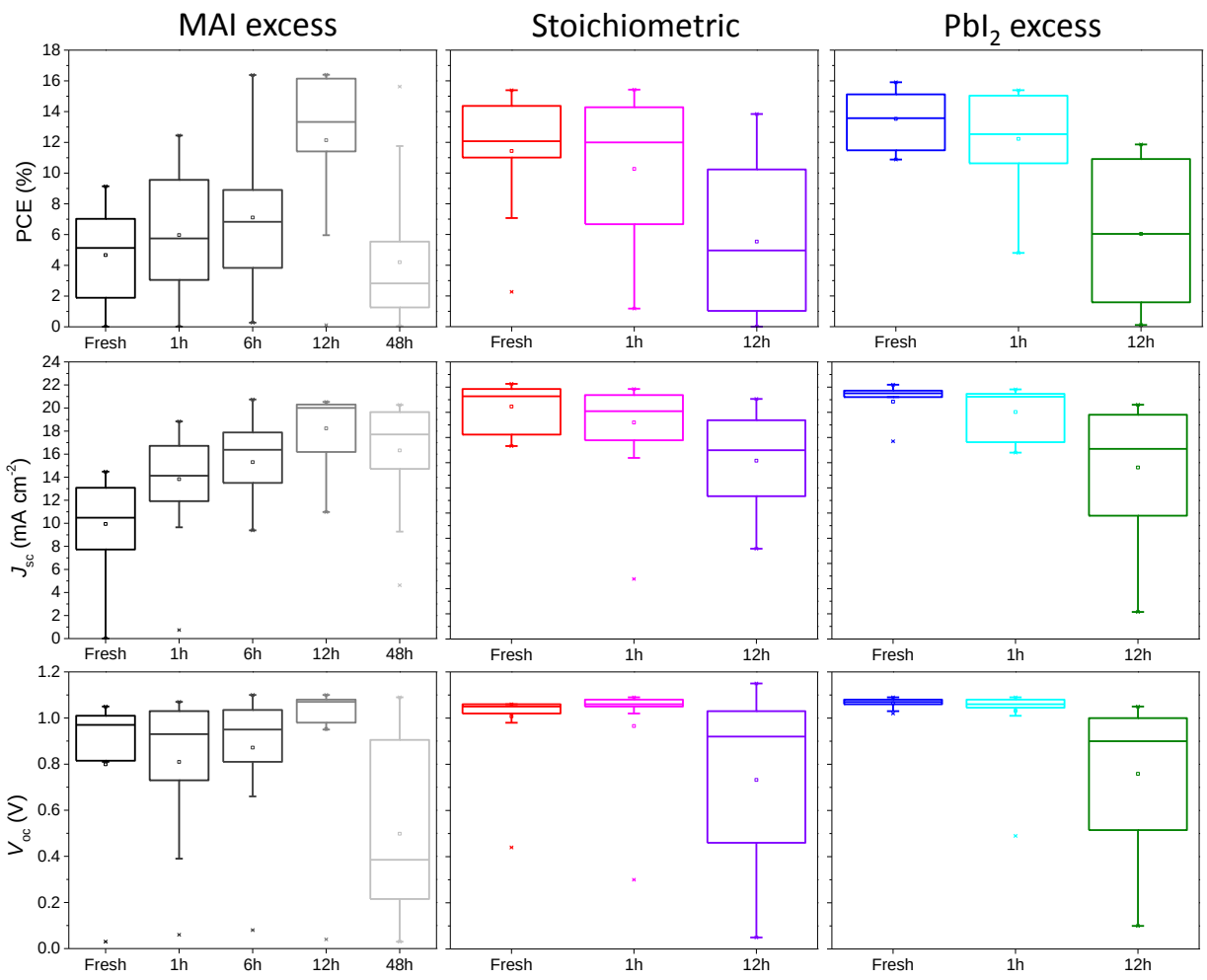

Figure 5. Photovoltaic performance of devices with different precursor ratios before and after hydration at 75% RH for different exposure times. The evaluation is based on the reverse J-V scans for a total of at least 18 individual devices for each type of perovskite film.

Remarkably, many of the devices comprising a perovskite layer prepared with an MAI excess exhibit increased PCE values after hydration followed by dehydration. After only 1 h exposure to 75% RH, we found a clear improvement of PCEs (Figure 5). This positive trend holds for even longer exposure times up to 12 h, eventually resulting in hero(ine) cell efficiencies comparable to the best performing devices derived from fresh stoichiometric or PbI_2-excess perovskite films, with an excellent stabilized power output (Figure S12 and S13). The increased performance mainly originates from an improvement in J_{sc}. Our XRD and SEM results provide evidence that this improvement in device performance can be correlated to the increase in crystallinity and reorientation of the perovskite crystals upon humidity exposure (Figure S14).[46] Yang *et al.* also report high efficiency devices with excess MAI in the perovskite layer after an air-annealing step to induce grain-coarsening and formation of large crystals.[23] Since the annealing step was performed under exposure to air, it is possible that this reported process is also moisture-assisted, which might be initiated already at room temperature. When the MAI-excess films are

exposed for longer times and/or at higher levels of humidity (*e.g.* 48 h at 75% RH), the monohydrated species of $MAPbI_3$ is formed, which appears as transparent flower-like crystals on the film. The drastic change in crystal morphology and structure is expected to result in pinholes and thus shunts, as well as in a loss in optical absorption and conductivity in the monohydrate regions.[20] This could explain the decrease in V_{oc} and in the overall photovoltaic performance of the degraded MAI-excess devices prepared in this study.

Despite the high PCEs that can be obtained by exposing MAI-excess films to humidified air, we note that these solar cells suffer from a significantly broader distribution in PCE compared to the PbI_2-excess devices. Further optimization of the moisture-induced recrystallization ("solvent annealing") process may allow higher reproducibility and device efficiencies.

To further investigate the causes of the observed differences in solar cell performance for the different precursor formulations, we analyzed the charge carrier lifetime and differential capacitance of the devices. For the PbI_2-excess and MAI-excess cases we also explored the influence of the hydration step. The experimental protocol for these measurements is reported by O'Regan *et al*. and is also presented in the supporting information for completeness.[47] In our analysis, the differential capacitance (dQ/dV_{oc} where Q is charge generated per unit area) is calculated from the solar cells' electrical response upon pulsed LED illumination. It is determined from the ratio between the J_{sc} during the pulse, dQ/dt (without background light bias), and the initial positive slope of the open-circuit photovoltage transient, dV_{oc}/dt, at each background light intensity measured after stabilization (see Figure S15). This approach yields capacitance values which account only for the movement of electronic charge, but we expect the quasi steady-state distribution of ionic charge in the device to be different for each background light intensity. For solar cells where the charge collection efficiency is less than 100%, this approach is prone to errors since the photocurrent during a pulse will not represent the full charge generation rate. We present the details of this limitation in the supporting information (Figure S16), where we also show that the conclusions drawn from the comparison of different devices in the following paragraphs is still representative and meaningful.

Figure 6a shows the differential capacitance versus V_{oc} for all devices. In Figures 6b and 6c we present the effect of hydration on carrier lifetime for MAI-excess and PbI_2-excess samples respectively (data points for the stoichiometric devices are also included).

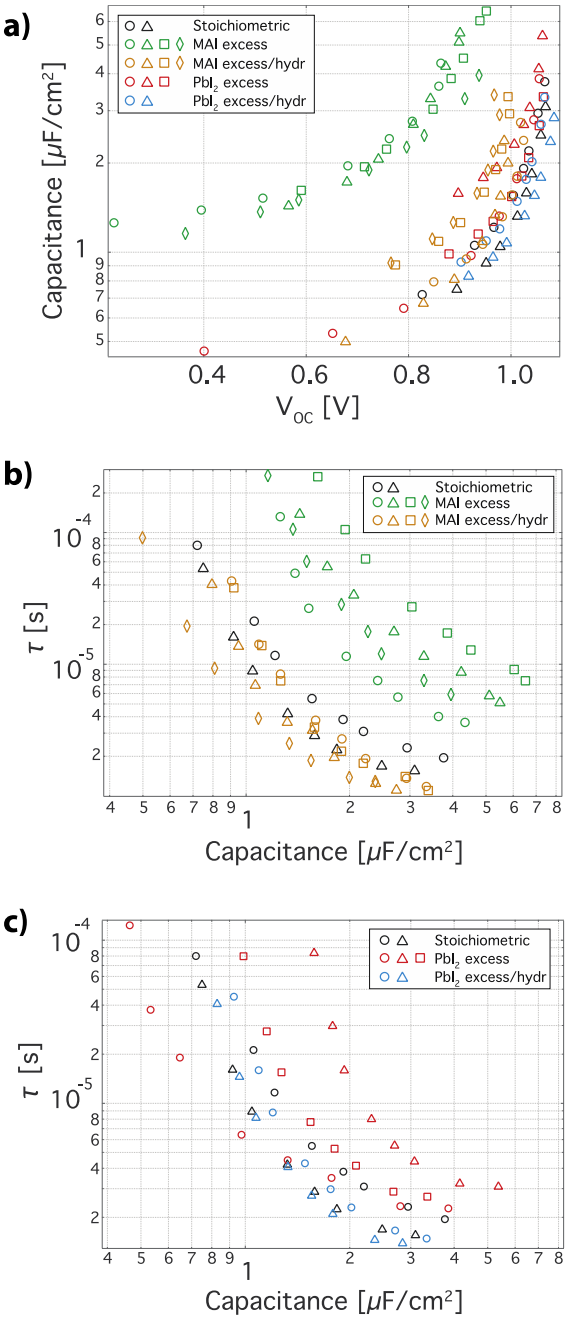

Figure 6. Optoelectronic transient measurements at different light intensities for stoichiometric, PbI_2-excess, MAI-excess, hydrated PbI_2-excess and hydrated MAI-excess devices. (a) Differential capacitance versus V_{oc}. (b-c) Lifetime extracted from photovoltage transients at open-circuit versus differential capacitance for (b) MAI-excess and (c) PbI_2-excess solar cells. Different symbols with the same color correspond to devices prepared with the same precursor ratio.

The key observation from Figure 6a is that the MAI-excess devices show a significantly higher differential capacitance as a function of V_{oc} relative to the stoichiometric and the PbI_2-excess devices. This difference can be interpreted as a variation in the density of electronic states (chemical capacitance) of cells prepared from different precursor solutions as a function of the Fermi level splitting in the device. The results can be interpreted in two possible ways: (1) the active layers fabricated with an MAI excess result in films with a higher density of traps states for a given V_{oc} or (2) the shift in the capacitance versus V_{oc} is related to a change in the interfacial energetics. In case 2, a variation in the active layer composition could give rise to dipole formation at the perovskite/TiO_2 and perovskite/spiro-OMeTAD interfaces, resulting in a lower effective built-in potential (V_{bi}) and reduced V_{oc} for a given light intensity. While a horizontal shift to lower V_{oc} values would be expected in this case, a reduced V_{bi} cannot account for the difference in slope of capacitance versus V_{oc} for the MAI-excess devices. Therefore, explanation 2 is unlikely to be dominant. A higher density of trap states corresponding to explanation 1 is consistent with the smaller crystal sizes observed in these films.

Strikingly, hydrating (or moisture annealing) the MAI-excess films before completing the devices resulted in capacitance versus V_{oc} relations that closely match the stoichiometric and PbI_2-excess cases. This reduction in capacitance is consistent with the structural analysis and device performance trend described in the previous sections. Figure 6a also shows that hydration of the PbI_2-excess perovskite films does not lead to a significant change in capacitance versus V_{oc} and that both these devices approximately resemble the behavior observed for the stoichiometric case.

Figure 6b displays transient photovoltage lifetimes as a function of differential capacitance for the MAI-excess devices with or without the hydration step. Photovoltage lifetimes are often used to assess the relative recombination rate constants in devices,[48] however care must be taken interpreting the values if the energetic distribution of electronic states varies between devices,[20] as is the case here. Once again, the MAI-excess devices exhibit distinctly different behavior from the stoichiometric control. Analogous to the data displayed in Figure 6a, the hydration step results in solar cells with remarkably similar photovoltage decay times as a function of capacitance to the stoichiometric case. We note that changes in interfacial energetics at the electrodes' interface and V_{bi} between solar cells fabricated with different precursor ratios would not significantly affect the lifetime versus capacitance characteristics, further evidence that explanation 2 is unlikely. On the other hand, a difference in the degree of energetic disorder within the film (explanation 1) could explain this observation. A higher density of trap states and associated chemical capacitance could increase the observed photovoltage relaxation time constant without significantly accelerating the charge recombination processes. This picture involves trap states which do not act as fast recombination centers (similar to dye sensitized solar cells).[49] We hypothesize that these traps may be present in MAI-rich regions surrounding the perovskite grains. These would inhibit electronic charge transport in MAI-excess devices, resulting in decreased collection efficiency and explaining the lower J_{sc} measured for these devices.

Finally, Figure 6c displays the trend of lifetimes observed for PbI_2-excess samples. These devices show longer lifetimes compared to the stoichiometric solar cells, consistent with the fractionally higher V_{oc} values. However, this difference is within statistical uncertainty. In a similar way to the hydrated MAI-

excess samples, hydration of PbI_2-excess devices yields a trend in lifetime versus differential capacitance that closely matches the stoichiometric control.

Conclusion

In conclusion, we performed both *in-situ* XRD and optoelectronic measurements to reveal the effects of moisture on $MAPbI_3$ perovskite films and solar cells derived from non-stoichiometric precursor solutions. Our findings indicate that the moisture stability of the perovskite film can be slightly improved by adding an excess of PbI_2 to the precursor solution. We assign the decelerated degradation process either to a PbI_2 layer formed at the grain boundaries during film crystallization or to the termination of the perovskite crystal with lead and iodine atoms, both of which would function as a barrier towards moisture ingress. In contrast, perovskite films containing an initial MAI excess first recrystallize upon exposure to humidified air at room temperature, resulting in large crystals with a preferential (110) orientation, before degradation occurs. Solar cells comprising an MAI-excess film initially show poor photovoltaic performance which we attribute to a high density of trapping states and energetic disorder in MAI-rich regions at perovskite grain boundaries, inferred from differential capacitance measurements. These states are likely to impede charge collection, explaining the lower J_{sc} in the fresh MAI-excess devices as well as longer photovoltage decay times than the other devices. However, when these films are exposed to moisture prior to applying the top electrodes, we observe an impressive improvement in PCE. We attribute this to the recrystallization of the perovskite and a concomitant reduction in electronic disorder to the level observed in the stoichiometric or PbI_2-excess devices. Our results shed light on the role of moisture in the processing and degradation of non-stoichiometric perovskite films, and indicate a procedure in which water vapor can be used to improve the device performance by solvent annealing.

Acknowledgements

The authors acknowledge Dr. Steffen Schmidt for the preparation of the SEM images and Prof. Thomas Bein and Johannes Schlipf for valuable discussions. The authors acknowledge funding from the German Federal Ministry of Education and Research (BMBF) under the agreement number 0SF0516B, the Bavarian Ministry of the Environment and Consumer Protection, the Bavarian Network “Solar Technologies Go Hybrid”, and the DFG Excellence Cluster Nanosystems Initiative Munich (NIM). P. D. acknowledges support from the European Union through the award of a Marie Curie Intra-European Fellowship. P. C., D. M. and P. B. are grateful to the UK Engineering and Physical Sciences Research Council for financial support (grants EP/J002305/1, EP/M025020/1, EP/G037515/1 and EP/M014797/1).

References

[1] “NREL Best Research-Cell Photovoltaic Efficiency Chart.,” can be found under http://www.nrel.gov/ncpv/images/efficiency_chart.jpg, **2016**.

[2] M. A. Green, K. Emery, Y. Hishikawa, W. Warta, E. D. Dunlop, *Prog. Photovoltaics Res. Appl.* **2016**, *24*, 905–913.

[3] A. Kojima, K. Teshima, Y. Shirai, T. Miyasaka, *J. Am. Chem. Soc.* **2009**, *131*, 6050–6051.

[4] G. Hodes, *Science* **2013**, *342*, 317–8.

[5] M. Liu, M. B. Johnston, H. J. Snaith, *Nature* **2013**, *501*, 395–8.

[6] A. Binek, M. L. Petrus, N. Huber, H. Bristow, Y. Hu, T. Bein, P. Docampo, *ACS Appl. Mater. Interfaces* **2016**, *8*, 12881–12886.

[7] M. L. Petrus, T. Bein, T. J. Dingemans, P. Docampo, *J. Mater. Chem. A* **2015**, *3*, 12159–12162.

[8] T. M. Schmidt, T. T. Larsen-Olsen, J. E. Carlé, D. Angmo, F. C. Krebs, *Adv. Energy Mater.* **2015**, *5*, n/a.

[9] G. Niu, X. Guo, L. Wang, *J. Mater. Chem. A* **2015**, *3*, 8970–8980.

[10] Y. Han, S. Meyer, Y. Dkhissi, K. Weber, J. M. Pringle, U. Bach, L. Spiccia, Y.-B. Cheng, *J. Mater. Chem. A* **2015**, *3*, 8139–8147.

[11] S. N. Habisreutinger, T. Leijtens, G. E. Eperon, S. D. Stranks, R. J. Nicholas, H. J. Snaith, *Nano Lett.* **2014**, *14*, 5561–5568.

[12] Z. Song, A. Abate, S. C. Watthage, G. K. Liyanage, A. B. Phillips, U. Steiner, M. Graetzel, M. J. Heben, *Adv. Energy Mater.* **2016**, 1600846.

[13] T. A. Berhe, W.-N. Su, C.-H. Chen, C.-J. Pan, J.-H. Cheng, H.-M. Chen, M.-C. Tsai, L.-Y. Chen, A. A. Dubale, B.-J. Hwang, *Energy Environ. Sci.* **2016**, *9*, 323–356.

[14] Y. Hu, J. Schlipf, M. Wussler, M. L. Petrus, W. Jaegermann, T. Bein, P. Müller-Buschbaum, P. Docampo, *ACS Nano* **2016**, *10*, 5999–6007.

[15] J. Yang, B. D. Siempelkamp, D. Liu, T. L. Kelly, *ACS Nano* **2015**, *9*, 1955–1963.

[16] X. Dong, X. Fang, M. Lv, B. Lin, S. Zhang, J. Ding, N. Yuan, *J. Mater. Chem. A* **2015**, *3*, 5360–5367.

[17] A. M. A. Leguy, Y. Hu, M. Campoy-Quiles, M. I. Alonso, O. J. Weber, P. Azarhoosh, M. van Schilfgaarde, M. T. Weller, T. Bein, J. Nelson, et al., *Chem. Mater.* **2015**, *27*, 3397–3407.

[18] L. Hu, G. Shao, T. Jiang, D. Li, X. Lv, H. Wang, X. Liu, H. Song, J. Tang, H. Liu, *ACS Appl. Mater. Interfaces* **2015**, *7*, 25113–25120.

[19] J. M. Frost, K. T. Butler, F. Brivio, C. H. Hendon, M. van Schilfgaarde, A. Walsh, *Nano Lett.* **2014**, *14*, 2584–2590.

[20] A. P. McMahon, N. P. Gallop, M. Acharya, M. Naderi, D. Williams, X. Li, N. M. Harrison, P. R. F. Barnes, *Thermodynamic Stability of Hydrated Hybrid Perovskites (under Review)*, **2016**.

[21] J. A. Christians, P. A. Miranda Herrera, P. V Kamat, *J. Am. Chem. Soc.* **2015**, *137*, 1530–1538.

[22] D. Li, S. A. Bretschneider, V. W. Bergmann, I. M. Hermes, J. Mars, A. Klasen, H. Lu, W. Tremel, M. Mezger, H.-J. Butt, et al., *J. Phys. Chem. C* **2016**, *120*, 6363–6368.

[23] M. Yang, Y. Zhou, Y. Zeng, C.-S. Jiang, N. P. Padture, K. Zhu, *Adv. Mater.* **2015**, *27*, 6363–70.

[24] C. Roldan-Carmona, P. Gratia, I. Zimmermann, G. Grancini, P. Gao, M. Graetzel, M. K. Nazeeruddin, *Energy Environ. Sci.* **2015**, *8*, 3550–3556.

[25] D. Bi, W. Tress, M. I. Dar, P. Gao, J. Luo, C. Renevier, K. Schenk, A. Abate, F. Giordano, J.-P. Correa Baena, et al., *Sci. Adv.* **2016**, *2*.

[26] M. Saliba, T. Matsui, J.-Y. Seo, K. Domanski, J.-P. Correa-Baena, N. Mohammad K., S. M. Zakeeruddin, W. Tress, A. Abate, A. Hagfeldt, et al., *Energy Environ. Sci.* **2016**.

[27] M. Saliba, S. Orlandi, T. Matsui, S. Aghazada, M. Cavazzini, J.-P. Correa-Baena, P. Gao, R. Scopelliti, E. Mosconi, K.-H. Dahmen, et al., *Nat. Energy* **2016**, *1*, 15017.

[28] T. Malinauskas, M. Saliba, T. Matsui, M. Daskeviciene, S. Urnikaite, P. Gratia, R. Send, H. Wonneberger, I. Bruder, M. Graetzel, et al., *Energy Environ. Sci.* **2016**, *9*, 1681–1686.

[29] Q. Chen, H. Zhou, T.-B. Song, S. Luo, Z. Hong, H.-S. Duan, L. Dou, Y. Liu, Y. Yang, *Nano Lett.* **2014**, *14*, 4158–4163.

[30] L. Wang, C. McCleese, A. Kovalsky, Y. Zhao, C. Burda, *J. Am. Chem. Soc.* **2014**, *136*, 12205–12208.

[31] F. Liu, Q. Dong, M. K. Wong, A. B. Djurišić, A. Ng, Z. Ren, Q. Shen, C. Surya, W. K. Chan, J. Wang, et al., *Adv. Energy Mater.* **2016**, *6*, n/a–n/a.

[32] D. H. Cao, C. C. Stoumpos, C. D. Malliakas, M. J. Katz, O. K. Farha, J. T. Hupp, M. G. Kanatzidis, *APL Mater.* **2014**, *2*, 091101.

[33] H. Zhang, J. Mao, H. He, D. Zhang, H. L. Zhu, F. Xie, K. S. Wong, M. Grätzel, W. C. H. Choy, *Adv. Energy Mater.* **2015**, *5*, n/a–n/a.

[34] T. J. Jacobsson, J.-P. Correa-Baena, E. Halvani Anaraki, B. Philippe, S. D. Stranks, M. E. F. Bouduban, W. Tress, K. Schenk, J. Teuscher, J.-E. Moser, et al., *J. Am. Chem. Soc.* **2016**, *138*, 10331–10343.

[35] D.-Y. Son, J.-W. Lee, Y. J. Choi, I.-H. Jang, S. Lee, P. J. Yoo, H. Shin, N. Ahn, M. Choi, D. Kim, et al., *Nat. Energy* **2016**, *1*, 16081.

[36] H. Dosch, B. W. Batterman, D. C. Wack, *Phys. Rev. Lett.* **1986**, *56*, 1144–1147.

[37] W. Zhang, M. Saliba, D. T. Moore, S. K. Pathak, M. T. Hörantner, T. Stergiopoulos, S. D. Stranks, G. E. Eperon, J. A. Alexander-Webber, A. Abate, et al., *Nat Commun* **2015**, *6*.

[38] N. J. Jeon, J. H. Noh, Y. C. Kim, W. S. Yang, S. Ryu, S. Il Seok, *Nat. Mater.* **2014**, *13*, 897–903.

[39] N. Ahn, D.-Y. Son, I.-H. Jang, S. M. Kang, M. Choi, N.-G. Park, *J. Am. Chem. Soc.* **2015**, *137*, 8696–8699.

[40] E. Mosconi, J. M. Azpiroz, F. De Angelis, *Chem. Mater.* **2015**, *27*, 4885–4892.

[41] C.-J. Tong, W. Geng, Z.-K. Tang, C.-Y. Yam, X.-L. Fan, J. Liu, W.-M. Lau, L.-M. Liu, *J. Phys. Chem. Lett.* **2015**, *6*, 3289–3295.

[42] T. Leijtens, G. E. Eperon, S. Pathak, A. Abate, M. M. Lee, H. J. Snaith, *Nat. Commun.* **2013**, *4*.

[43] G. Niu, W. Li, F. Meng, L. Wang, H. Dong, Y. Qiu, *J. Mater. Chem. A* **2014**, *2*, 705–710.

[44] X. Zhu, H. Sun, D. Yang, P. Wangyang, X. Gao, *J. Mater. Sci. Mater. Electron.* **2016**, 1–6.

[45] S. H. and Z. X. and Y. D. and H. Z. and Z. S. and Z. Beijun, *J. Semicond.* **2012**, *33*, 53002.

[46] F. Hanusch, M. Petrus, P. Docampo, in *Unconv. Thin Film Photovoltaics*, The Royal Society Of Chemistry, **2016**, pp. 32–56.

[47] B. C. O'Regan, P. R. F. Barnes, X. Li, C. Law, E. Palomares, J. M. Marin-Beloqui, *J. Am. Chem. Soc.* **2015**, *137*, 5087–5099.

[48] V. Roiati, S. Colella, G. Lerario, L. De Marco, A. Rizzo, A. Listorti, G. Gigli, *Energy Environ. Sci.* **2014**, *7*, 1889–1894.

[49] P. R. F. Barnes, K. Miettunen, X. Li, A. Y. Anderson, T. Bessho, M. Gratzel, B. C. O'Regan, *Adv. Mater.* **2013**, *25*, 1881–922.

Table of content Figure:

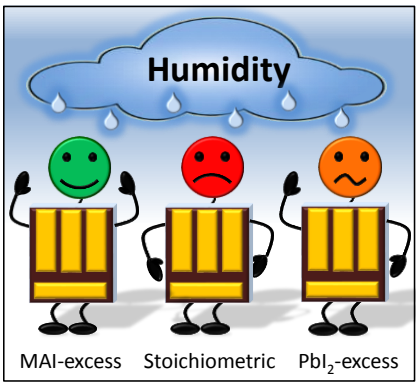

Table of content text:

We studied the effect of moisture on hybrid perovskite films and solar cells prepared from non-stoichiometric precursor solutions. A small PbI_2 excess was found to decelerate moisture-induced degradation compared to stoichiometric samples. MAI-excess devices with initially poor efficiencies showed a remarkable increase in performance after exposure to moisture due to a recrystallization process.